On the inertially decoupled structure of the floating base robot dynamics ⋆

Gianluca Garofalo * **Bernd Henze** * **Johannes Englsberger** * **Christian Ott** *

* *Institute of Robotics and Mechatronics, German Aerospace Center (DLR), Wessling, Germany (e-mail: gianluca.garofalo(at)dlr.de).*

Abstract: In this paper a coordinate transformation is proposed that provides an inertially decoupled structure for the equations of motion of a floating base robot. As the center of mass (CoM) has been used both for locomotion and balancing of legged robots because of its decoupled dynamics from the rest of the system, we expect to benefit from our coordinate transformation since it allows to separate the linear and angular centroidal dynamics from the joint dynamics. Gaining insights about the model, simpler and more effective control laws can be developed. As an example of application, the proposed transformation is used in the derivation of a humanoid balance controller.

Keywords: Robotics, Dynamics, Co-ordinate transformations, Conservation of momentum, Humanoid balance controller.

1. INTRODUCTION

The increasing complexity of the robotic systems has, since decades, encouraged researchers all over the world to analyze the dynamic equations of motion of the robot to improve the computational efficiency and gain insights that might lead to more effective control laws.

From the numeric computation point of view, some of the milestones are the results provided in Uicker (1965); Stepanenko and Vukobratovic (1976) where the recursive Newton-Euler algorithm was formulated and in Orin et al. (1979) where a more efficient version was presented. In Hollerbach (1980) it was shown that not only the Newton-Euler approach, but also the Lagrangian formulation could provide an equally efficient algorithm and in Silver (1982) the equivalence of the two methods was provided. While the previous works deal with the inverse dynamics problem, in Vereshchagin (1974) the direct one is considered, so that in the end for both problems algorithms with $O(n)$ complexity are available. On the other hand, recently the introduction of flexible joint robots has risen the need of computing the derivatives with respect to time of all the matrices of the dynamic model, as it is shown in Spong (1987); De Luca and Flacco (2011); Ott (2008). The solution of other problems and analysis requires, instead, to differentiate the matrices with respect to the state or the dynamic parameters. The controllability analysis of underactuated manipulators motivated in Müller (2007) to provide an efficient factorization for the inverse of the inertia matrix, in order to compute its partial derivatives. The derivative with respect to the state of the direct and inverse dynamic function, useful in optimization problems or in state estimation problems, were provided in Suleiman et al. (2008); Sohl and Bobrow (2001). Finally, in Garofalo et al. (2013) a summary and an algorithm to compute the derivatives of each matrix of the dynamic model with respect to time, state and dynamic parameters, was provided.

Insights about the structure of the equations have turned out to be of great usefulness when dealing with floating base robots. In the field of space robotics the results presented in Umetani and Yoshida (1987, 1989), where the generalized Jacobian matrix was introduced for the first time, are often used. The idea is to replace the floating base velocity in the computation of the end-effector Jacobian matrix with the generalized momentum of the system which, in case of space operations, is often zero or at least constant. This allows to obtain a simpler expression, i.e. the generalized Jacobian matrix. In the field of legged balancing, control laws that directly take advantage of the property of the equations of motion have been proposed in Hyon et al. (2007); Ott et al. (2011); Henze et al. (2014). What is presented here goes in this direction; providing a coordinate transformation that can lead to more efficient and effective control laws making use of the intrinsic properties of the system model. Knowing that the conservation of the generalized momentum is implicitly contained in the dynamic equations of a floating base robot, as shown in Wieber (2006) for legged robots, we propose a coordinate transformation inspired by the combination of the results from Orin et al. (2013) and Ott et al. (2008). We show that the conservation of momentum directly implies orthogonality relationships between some of the matrices of the dynamic model. These can be used to perform a coordinate transformation that leads to inertially decoupled equations, since in the new coordinates the transformed inertia matrix will be block diagonal. The results presented here include and extend those in Hyon et al. (2007); Ott et al. (2011), allowing to separate the linear and angular centroidal dynamics from the joint dynamics.

⋆ This research is partly supported by the Initiative and Networking Fund of the Helmholtz Association through a Helmholtz Young Investigators Group (Grant no. VH-NG-808).

The paper is organized as follows: in Section 2 we describe the model and provide all the properties required to obtain the main result of the paper, which is derived and presented in Section 3. Section 4 considers the relationships with some of the works present in literature, while Section 5 shows an example of application of the proposed coordinate transformation, along with the advantages compared to previous results. Finally, Section 6 concludes our work with a short discussion and outline of future work.

2. PRELIMINARIES

We will consider floating base robots, for which the state is defined by the variables $\boldsymbol{x}$ and $\boldsymbol{v}$, being $\boldsymbol{x}$ the complete configuration coordinates with dimension n_v and $\boldsymbol{v} \in \mathbb{R}^{n_v}$ the complete velocity coordinates, i.e. including both the floating base and joint coordinates. Note that in general $\boldsymbol{x}$ might not necessarily have all entries in $\mathbb{R}$ and

$$\dot{\boldsymbol{x}} \neq \boldsymbol{v} \ ,$$

which is the case when, for example, the rotation matrix is used to represent the orientation. Indicating with $\boldsymbol{\tau} \in \mathbb{R}^{n_q}$ the torques provided by the motors and with $\boldsymbol{w}_i \in \mathbb{R}^6$ one of the m contact wrenches, then the dynamic model can be written as

$$\boldsymbol{M}(\boldsymbol{x})\dot{\boldsymbol{v}} + \boldsymbol{C}(\boldsymbol{x},\boldsymbol{v})\boldsymbol{v} + \boldsymbol{g}(\boldsymbol{x}) = \boldsymbol{Q}^T\boldsymbol{\tau} + \sum_{i=1}^{m} \boldsymbol{J}_i^T(\boldsymbol{x})\boldsymbol{w}_i \ , \quad (1)$$

where $\boldsymbol{M}(\boldsymbol{x}) \in \mathbb{R}^{n_v \times n_v}$ is the positive definite inertia matrix, $\boldsymbol{C}(\boldsymbol{x},\boldsymbol{v}) \in \mathbb{R}^{n_v \times n_v}$ is the Coriolis matrix and $\boldsymbol{g}(\boldsymbol{x}) \in \mathbb{R}^{n_v}$ is the vector of gravity torques. Each $\boldsymbol{J}_i^T(\boldsymbol{x})$ maps the correspondent $\boldsymbol{w}_i$ to the generalized forces of the system, while $\boldsymbol{Q}$ is the matrix that selects the joint velocities $\dot{\boldsymbol{q}} \in \mathbb{R}^{n_q}$ out of all the velocity coordinates, i.e. $\dot{\boldsymbol{q}} = \boldsymbol{Q}\boldsymbol{v}$.

As it was firstly shown in Kajita et al. (2003), it is always possible to express the generalized momentum $\boldsymbol{h} \in \mathbb{R}^6$, i.e. the linear and the angular momentum stacked together, as

$$\boldsymbol{h} = \boldsymbol{A}(\boldsymbol{x})\boldsymbol{v} \ , \quad (2)$$

where $\boldsymbol{A}(\boldsymbol{x})$ is called the centroidal momentum matrix in Orin et al. (2013) if the generalized momentum is expressed in a frame attached to the center of mass (CoM) and with the axis aligned with the inertial frame. In the following we will always assume that this is the case.

Since the linear momentum $\boldsymbol{p} \in \mathbb{R}^3$ is directly related to the velocity of the CoM $\dot{\boldsymbol{x}}_{CoM}$, i.e. $\boldsymbol{p} = m\dot{\boldsymbol{x}}_{CoM}$ where m is the total mass of the robot, it is clear that a relationship must exist between the centroidal momentum matrix $\boldsymbol{A}(\boldsymbol{x})$ and the Jacobian matrix $\boldsymbol{J}_{CoM}(\boldsymbol{x})$ mapping the velocity coordinates into the velocity of the CoM of the robot, i.e. $\dot{\boldsymbol{x}}_{CoM} = \boldsymbol{J}_{CoM}(\boldsymbol{x})\boldsymbol{v}$. To this end, we partition the centroidal momentum matrix as $\boldsymbol{A}(\boldsymbol{x}) = \left[\boldsymbol{A}_p^T(\boldsymbol{x}) \ \boldsymbol{A}_l^T(\boldsymbol{x})\right]^T$, so that

$$\boldsymbol{p} = \boldsymbol{A}_p(\boldsymbol{x})\boldsymbol{v} \quad (3)$$
$$\boldsymbol{l} = \boldsymbol{A}_l(\boldsymbol{x})\boldsymbol{v} \ , \quad (4)$$

where $\boldsymbol{l} \in \mathbb{R}^3$ is the angular momentum. Equating the two expressions of $\boldsymbol{p}$ it follows that

$$\boldsymbol{A}_p(\boldsymbol{x}) = m\boldsymbol{J}_{CoM}(\boldsymbol{x}) \ , \quad (5)$$

since the equality must be satisfied for every possible choice of $\boldsymbol{v}$. In view of (5) and knowing that $\boldsymbol{g}(\boldsymbol{x})$ is obtained from the mapping of the force $\boldsymbol{f}_g = m\, g\, \boldsymbol{e}_g$ through $\boldsymbol{J}_{CoM}^T(\boldsymbol{x})$, the gravity torques can be written as $\boldsymbol{g}(\boldsymbol{x}) = g\boldsymbol{A}_p^T(\boldsymbol{x})\boldsymbol{e}_g$, where g is the gravitational constant and $\boldsymbol{e}_g$ a unit vector pointing upwards.

For a system described by the dynamic model (1), it is well known that the following property holds

Proposition 1. (Newton−Euler equations). Let $\boldsymbol{w}_{CoM}$ be the total wrench acting at the CoM obtained from the combination of all the external wrenches, then

$$\dot{\boldsymbol{h}} = \boldsymbol{w}_{CoM} \ . \quad (6)$$

From the previous property and the expression of the generalized momentum given in (2), the following corollaries can be derived

Corollary 2. (Conservation of generalized momentum).

Let us assume that we have a free floating robot ($\boldsymbol{g}(\boldsymbol{x}) = \boldsymbol{0}$), with no external wrenches acting on it, then

$$\boldsymbol{A}(\boldsymbol{x})\dot{\boldsymbol{v}} + \dot{\boldsymbol{A}}(\boldsymbol{x},\boldsymbol{v})\boldsymbol{v} = \boldsymbol{0} \ . \quad (7)$$

Corollary 3. (Conservation of angular momentum).

Let us assume that the resulting total wrench at the CoM is a pure force, then

$$\boldsymbol{A}_l(\boldsymbol{x})\dot{\boldsymbol{v}} + \dot{\boldsymbol{A}}_l(\boldsymbol{x},\boldsymbol{v})\boldsymbol{v} = \boldsymbol{0} \ . \quad (8)$$

3. MAIN RESULT

The goal of this section is to find a coordinate transformation that can inertially decouple the equations of motion of a floating base robot, i.e. it transforms the inertia matrix into a block diagonal matrix. The transformation is based on orthogonality relationships between matrices. As we will show in the next subsections, these are direct consequences of basic mechanical principles and therefore have a clear physical interpretation. To easily derive the results, special cases are considered, although the results are valid in general.

3.1 Conservation of generalized momentum

Let us assume that we have a free floating robot with no external wrenches acting on it, so that the only torques are those provided by the motors. Replacing $\dot{\boldsymbol{v}}$ from (1) into (7) and setting $\boldsymbol{g}(\boldsymbol{x})$ and all the $\boldsymbol{w}_i$ to zero leads to

$$\begin{aligned}&\boldsymbol{A}(\boldsymbol{x})\boldsymbol{M}^{-1}(\boldsymbol{x})\boldsymbol{Q}^T\boldsymbol{\tau} + \\ &\quad - \left(\boldsymbol{A}(\boldsymbol{x})\boldsymbol{M}^{-1}(\boldsymbol{x})\boldsymbol{C}(\boldsymbol{x},\boldsymbol{v}) - \dot{\boldsymbol{A}}(\boldsymbol{x},\boldsymbol{v})\right)\boldsymbol{v} = \boldsymbol{0} \ .\end{aligned} \quad (9)$$

Equation (9) holds for every possible choice of $\boldsymbol{v}$ and $\boldsymbol{\tau}$, therefore it is clear that the following conditions must be satisfied

$$\boldsymbol{A}(\boldsymbol{x})\boldsymbol{M}^{-1}(\boldsymbol{x})\boldsymbol{Q}^T = \boldsymbol{0} \quad (10)$$
$$\left(\boldsymbol{A}(\boldsymbol{x})\boldsymbol{M}^{-1}(\boldsymbol{x})\boldsymbol{C}(\boldsymbol{x},\boldsymbol{v}) - \dot{\boldsymbol{A}}(\boldsymbol{x},\boldsymbol{v})\right)\boldsymbol{v} = \boldsymbol{0} \ . \quad (11)$$

Inspired by the velocity coordinate transformation used in Ott et al. (2008), we choose the following one

$$\boldsymbol{\xi} = \begin{bmatrix}\boldsymbol{h}\\ \dot{\boldsymbol{q}}\end{bmatrix} = \boldsymbol{A}_Q(\boldsymbol{x})\boldsymbol{v} \qquad \boldsymbol{A}_Q(\boldsymbol{x}) = \begin{bmatrix}\boldsymbol{A}(\boldsymbol{x})\\ \boldsymbol{Q}\end{bmatrix} \ , \quad (12)$$

with the inverse transformation given by [1]

[1] Given a matrix $\boldsymbol{T}$, we denote with $\boldsymbol{T}^{+_M}$ the dynamically consistent weighted pseudo inverse defined as $\boldsymbol{T}^{+_M}(\boldsymbol{x}) := \boldsymbol{M}^{-1}(\boldsymbol{x})\boldsymbol{T}^T\left(\boldsymbol{T}\boldsymbol{M}^{-1}(\boldsymbol{x})\boldsymbol{T}^T\right)^{-1}$.

$$\begin{aligned} \boldsymbol{v} &= \boldsymbol{A}_Q^{-1}(\boldsymbol{x})\boldsymbol{\xi} \\ \boldsymbol{A}_Q^{-1}(\boldsymbol{x}) &= \left[\boldsymbol{A}^{+_M}(\boldsymbol{x})\ \ \boldsymbol{Q}^{+_M}(\boldsymbol{x})\right] \ . \end{aligned} \tag{13}$$

Pre-multiplying (1) by $\boldsymbol{A}_Q^{-T}(\boldsymbol{x})$, using

$$\dot{\boldsymbol{v}} = \boldsymbol{A}_Q^{-1}(\boldsymbol{x})\left(\dot{\boldsymbol{\xi}} - \dot{\boldsymbol{A}}_Q(\boldsymbol{x})\boldsymbol{A}_Q^{-1}(\boldsymbol{x})\boldsymbol{\xi}\right) \tag{14}$$

and the orthogonality relationship expressed in (10) leads to the equations of motion in the new coordinates

$$\underbrace{\begin{bmatrix}\boldsymbol{\Lambda}_h(\boldsymbol{x}) & \boldsymbol{0}\\ \boldsymbol{0} & \boldsymbol{\Lambda}_q(\boldsymbol{x})\end{bmatrix}}_{\boldsymbol{\Lambda}(\boldsymbol{x})}\dot{\boldsymbol{\xi}} + \underbrace{\begin{bmatrix}\boldsymbol{\Gamma}_{hh}(\boldsymbol{x},\boldsymbol{v}) & \boldsymbol{\Gamma}_{hq}(\boldsymbol{x},\boldsymbol{v})\\ -\boldsymbol{\Gamma}_{hq}^T(\boldsymbol{x},\boldsymbol{v}) & \boldsymbol{\Gamma}_{qq}(\boldsymbol{x},\boldsymbol{v})\end{bmatrix}}_{\boldsymbol{\Gamma}(\boldsymbol{x},\boldsymbol{A}_Q^{-1}(\boldsymbol{x})\boldsymbol{\xi})}\boldsymbol{\xi} = \begin{bmatrix}\boldsymbol{0}\\ \boldsymbol{\tau}\end{bmatrix} \ , \tag{15}$$

where

$$\boldsymbol{\Lambda}_h(\boldsymbol{x}) = \left(\boldsymbol{A}(\boldsymbol{x})\boldsymbol{M}^{-1}(\boldsymbol{x})\boldsymbol{A}^T(\boldsymbol{x})\right)^{-1} \tag{16}$$

$$\boldsymbol{\Lambda}_q(\boldsymbol{x}) = \left(\boldsymbol{Q}\boldsymbol{M}^{-1}(\boldsymbol{x})\boldsymbol{Q}^T\right)^{-1} \tag{17}$$

$$\boldsymbol{\Gamma}(\boldsymbol{x},\boldsymbol{v})\boldsymbol{\xi} = \boldsymbol{\Lambda}(\boldsymbol{x})\begin{bmatrix}\boldsymbol{A}(\boldsymbol{x})\boldsymbol{M}^{-1}(\boldsymbol{x})\boldsymbol{C}(\boldsymbol{x},\boldsymbol{v}) - \dot{\boldsymbol{A}}(\boldsymbol{x},\boldsymbol{v})\\ \boldsymbol{Q}\boldsymbol{M}^{-1}(\boldsymbol{x})\boldsymbol{C}(\boldsymbol{x},\boldsymbol{v})\end{bmatrix}\boldsymbol{v} \ . \tag{18}$$

The latter shows that, although the generalized momentum will influence the joint dynamics through $\boldsymbol{\Gamma}(\boldsymbol{x},\boldsymbol{v})$ since in general $-\boldsymbol{\Gamma}_{hq}^T(\boldsymbol{x},\boldsymbol{v})\boldsymbol{h} \neq \boldsymbol{0}$, the inverse is not true. As a matter of fact, from (11) and (18) follows that

$$\boldsymbol{\Gamma}_{hh}(\boldsymbol{x},\boldsymbol{v})\boldsymbol{h} + \boldsymbol{\Gamma}_{hq}(\boldsymbol{x},\boldsymbol{v})\dot{\boldsymbol{q}} = \boldsymbol{0} \ , \tag{19}$$

which can be seen as a natural consequence of the conservation of the generalized momentum.

3.2 Conservation of angular momentum

In this subsection the structure is further explored to show additional inertial separation. The condition expressed in (10) can be interpreted in such a way that the torques produced by the motors are internal forces for the free floating robot and therefore they produce no change in the generalized momentum. Similarly, let us assume that the resulting total wrench at the CoM is a pure force $\boldsymbol{f}_{CoM}$, which maps via $\boldsymbol{J}_{CoM}^T(\boldsymbol{x})$. Replacing $\dot{\boldsymbol{v}}$ from (1) into (8) and setting $\boldsymbol{g}(\boldsymbol{x})$ and $\boldsymbol{\tau}$ to zero leads to

$$\begin{aligned} &\frac{1}{m}\boldsymbol{A}_l(\boldsymbol{x})\boldsymbol{M}^{-1}(\boldsymbol{x})\boldsymbol{A}_p^T(\boldsymbol{x})\boldsymbol{f}_{CoM} + \\ &\quad - \left(\boldsymbol{A}_l(\boldsymbol{x})\boldsymbol{M}^{-1}(\boldsymbol{x})\boldsymbol{C}(\boldsymbol{x},\boldsymbol{v}) - \dot{\boldsymbol{A}}_l(\boldsymbol{x},\boldsymbol{v})\right)\boldsymbol{v} = 0 \ , \end{aligned} \tag{20}$$

where, additionally, (5) has been used. This condition, holding for every possible choice of $\boldsymbol{v}$ and $\boldsymbol{f}_{CoM}$, leads to

$$\boldsymbol{A}_l(\boldsymbol{x})\boldsymbol{M}^{-1}(\boldsymbol{x})\boldsymbol{A}_p^T(\boldsymbol{x}) = \boldsymbol{0} \ . \tag{21}$$

In view of this orthogonality relationship, we conclude that $\boldsymbol{\Lambda}_h(\boldsymbol{x})$ is itself block diagonal. In particular,

$$\begin{aligned} \boldsymbol{\Lambda}_h(\boldsymbol{x}) &= \left(\begin{bmatrix}\boldsymbol{A}_p(\boldsymbol{x})\\ \boldsymbol{A}_l(\boldsymbol{x})\end{bmatrix}\boldsymbol{M}^{-1}(\boldsymbol{x})\left[\boldsymbol{A}_p^T(\boldsymbol{x})\ \ \boldsymbol{A}_l^T(\boldsymbol{x})\right]\right)^{-1} \\ &= \begin{bmatrix}\boldsymbol{\Lambda}_p(\boldsymbol{x}) & \boldsymbol{0}\\ \boldsymbol{0} & \boldsymbol{\Lambda}_l(\boldsymbol{x})\end{bmatrix} \end{aligned} \ , \tag{22}$$

with

$$\boldsymbol{\Lambda}_p(\boldsymbol{x}) = \left(\boldsymbol{A}_p(\boldsymbol{x})\boldsymbol{M}^{-1}(\boldsymbol{x})\boldsymbol{A}_p^T(\boldsymbol{x})\right)^{-1} \tag{23}$$

$$\boldsymbol{\Lambda}_l(\boldsymbol{x}) = \left(\boldsymbol{A}_l(\boldsymbol{x})\boldsymbol{M}^{-1}(\boldsymbol{x})\boldsymbol{A}_l^T(\boldsymbol{x})\right)^{-1} \ . \tag{24}$$

3.3 Final structure

Combining the results from the previous subsections, (1) can be written in the new coordinates as (omitting the dependencies)

$$\begin{aligned} \begin{bmatrix}\boldsymbol{\Lambda}_p & \boldsymbol{0} & \boldsymbol{0}\\ \boldsymbol{0} & \boldsymbol{\Lambda}_l & \boldsymbol{0}\\ \boldsymbol{0} & \boldsymbol{0} & \boldsymbol{\Lambda}_q\end{bmatrix}\dot{\boldsymbol{\xi}} + \begin{bmatrix}\boldsymbol{\Gamma}_{pp} & \boldsymbol{\Gamma}_{pl} & \boldsymbol{\Gamma}_{pq}\\ -\boldsymbol{\Gamma}_{pl}^T & \boldsymbol{\Gamma}_{ll} & \boldsymbol{\Gamma}_{lq}\\ -\boldsymbol{\Gamma}_{pq}^T & -\boldsymbol{\Gamma}_{lq}^T & \boldsymbol{\Gamma}_{qq}\end{bmatrix}\boldsymbol{\xi} + \begin{bmatrix}g\,\boldsymbol{e}_g\\ \boldsymbol{0}\\ \boldsymbol{0}\end{bmatrix} \\ = \begin{bmatrix}\boldsymbol{0}\\ \boldsymbol{0}\\ \boldsymbol{\tau}\end{bmatrix} + \sum_i \bar{\boldsymbol{J}}_i^T\boldsymbol{w}_i \end{aligned} \ , \tag{25}$$

where $\bar{\boldsymbol{J}}_i(\boldsymbol{x}) = \boldsymbol{J}_i(\boldsymbol{x})\boldsymbol{A}_Q^{-1}(\boldsymbol{x})$, and the result from Appendix A and the orthogonality relationship expressed in (21) have been used to obtain

$$\boldsymbol{A}_Q^{-T}(\boldsymbol{x})\boldsymbol{g}(\boldsymbol{x}) = \begin{bmatrix}\boldsymbol{A}_p^{+_M T}(\boldsymbol{x})\\ \boldsymbol{A}_l^{+_M T}(\boldsymbol{x})\\ \boldsymbol{Q}^{+_M T}(\boldsymbol{x})\end{bmatrix} g\boldsymbol{A}_p^T(\boldsymbol{x})\boldsymbol{e}_g = \begin{bmatrix}g\,\boldsymbol{e}_g\\ \boldsymbol{0}\\ \boldsymbol{0}\end{bmatrix} \ . \tag{26}$$

The result can be further refined. Let us assume that no contact wrenches are acting on the system. Setting each of the $\boldsymbol{w}_i$ to zero and taking into account (19), the first three lines of the model are

$$\boldsymbol{\Lambda}_p(\boldsymbol{x})\dot{\boldsymbol{p}} = -g\,\boldsymbol{e}_g \ . \tag{27}$$

On the other hand, from (6) it follows that $\dot{\boldsymbol{p}} = -m\,g\,\boldsymbol{e}_g$ must hold. Comparing the two expressions of $\dot{\boldsymbol{p}}$, we conclude that

$$\boldsymbol{\Lambda}_p = \frac{1}{m}\boldsymbol{E}_3 \ , \tag{28}$$

where $\boldsymbol{E}_3$ is the 3×3 identity matrix. Note that, because of the passivity property, it also follows that $\boldsymbol{\Gamma}_{pp}(\boldsymbol{x},\boldsymbol{v})$ is skew-symmetric. Obviously a similar result holds in terms of $\boldsymbol{J}_{CoM}(\boldsymbol{x})$. In particular, we get the identity

$$\boldsymbol{J}_{CoM}(\boldsymbol{x})\boldsymbol{M}^{-1}(\boldsymbol{x})\boldsymbol{J}_{CoM}^T(\boldsymbol{x}) = \frac{1}{m}\boldsymbol{E}_3 \ , \tag{29}$$

which provides an explanation for the structure obtained after the coordinate transformation used in Hyon et al. (2007); Ott et al. (2011); Henze et al. (2014) and shown in Section 5.

Fact 4. In view of (5), $\frac{1}{m}\boldsymbol{A}_p^T(\boldsymbol{x})$ allows to map a force at the CoM to the generalized forces of the model. We can generalize the result and look for the matrix $\boldsymbol{T}(\boldsymbol{x})$ whose transpose allows to map a wrench $\boldsymbol{w}_{CoM}$ acting at the CoM, i.e.

$$\boldsymbol{M}(\boldsymbol{x})\dot{\boldsymbol{v}} + \boldsymbol{C}(\boldsymbol{x},\boldsymbol{v})\boldsymbol{v} = \boldsymbol{T}^T(\boldsymbol{x})\boldsymbol{w}_{CoM} \ . \tag{30}$$

Performing the coordinate transformation and considering only the first six lines, we get

$$\boldsymbol{\Lambda}_h(\boldsymbol{x})\dot{\boldsymbol{h}} = \boldsymbol{A}^{+_M T}(\boldsymbol{x})\boldsymbol{T}^T(\boldsymbol{x})\boldsymbol{w}_{CoM} \ , \tag{31}$$

where (19) has been used. Since (6) must hold, we obtain

$$\boldsymbol{T}^T(\boldsymbol{x}) = \boldsymbol{A}^T(\boldsymbol{x})\boldsymbol{\Lambda}_h(\boldsymbol{x}) = \left[\boldsymbol{A}_p^T(\boldsymbol{x})\boldsymbol{\Lambda}_p(\boldsymbol{x})\ \ \boldsymbol{A}_l^T(\boldsymbol{x})\boldsymbol{\Lambda}_l(\boldsymbol{x})\right] \ , \tag{32}$$

which includes the already known result for the mapping of a force at the CoM.

It is important to notice that the physical units of the first six equations and the remaining ones are not the same. This is not surprising, since we use a mix of velocities and generalized momentum as part of the new state.

4. RELATED WORKS

In this section we consider the relationships with some of the works present in literature. In particular, we will show that our formulation implicitly contains the well known concept of generalized Jacobian matrix and additionally allows to write the kinetic energy of the system as a sum of three contributions.

4.1 The generalized Jacobian matrix

Let $\dot{\boldsymbol{x}}_e$ be the velocity of the end-effector and $J_e(\boldsymbol{x})$ the associated Jacobian matrix, so that

$$\dot{\boldsymbol{x}}_e = \boldsymbol{J}_e(\boldsymbol{x})\boldsymbol{v} = \boldsymbol{J}_e(\boldsymbol{x})\boldsymbol{A}_Q^{-1}(\boldsymbol{x})\boldsymbol{\xi} \ ,$$

expressed in terms of both the old and new coordinates. If $\boldsymbol{h} = \boldsymbol{0}$ and we take into account the expression of $\boldsymbol{A}_Q^{-1}(\boldsymbol{x})$, the previous expression simplifies to

$$\begin{aligned} \dot{\boldsymbol{x}}_e &= \bar{\boldsymbol{J}}_e(\boldsymbol{x})\dot{\boldsymbol{q}} \\ \bar{\boldsymbol{J}}_e(\boldsymbol{x}) &= \boldsymbol{J}_e(\boldsymbol{x})\boldsymbol{Q}^{+_M}(\boldsymbol{x}) \ . \end{aligned}$$

Partitioning the inertia matrix and the end-effector Jacobian matrix to separate the role of the floating base from the joints, i.e.

$$\begin{aligned} \boldsymbol{M}(\boldsymbol{x}) &= \begin{bmatrix} \boldsymbol{M}_b(\boldsymbol{x}) & \boldsymbol{M}_c(\boldsymbol{x}) \\ \boldsymbol{M}_c^T(\boldsymbol{x}) & \boldsymbol{\Lambda}_q(\boldsymbol{x}) \end{bmatrix} \\ \boldsymbol{J}_e(\boldsymbol{x}) &= \left[\boldsymbol{J}_{eb}(\boldsymbol{x}) \ \ \boldsymbol{J}_{eq}(\boldsymbol{x})\right] \ , \end{aligned}$$

the following expressions are obtained by direct computation

$$\begin{aligned} \boldsymbol{Q}^{+_M}(\boldsymbol{x}) &= \begin{bmatrix} -\boldsymbol{M}_b^{-1}(\boldsymbol{x})\boldsymbol{M}_c(\boldsymbol{x}) \\ \boldsymbol{E}_{n_q} \end{bmatrix} \\ \bar{\boldsymbol{J}}_e(\boldsymbol{x}) &= \boldsymbol{J}_{eq}(\boldsymbol{x}) - \boldsymbol{J}_{eb}(\boldsymbol{x})\boldsymbol{M}_b^{-1}(\boldsymbol{x})\boldsymbol{M}_c(\boldsymbol{x}) \ , \end{aligned} \qquad (33)$$

where $\boldsymbol{E}_{n_q}$ is the $n_q \times n_q$ identity matrix and (33) is the well know definition of generalized Jacobian matrix introduced in Umetani and Yoshida (1987, 1989).

4.2 The average velocity

In Orin et al. (2013) the centroidal momentum matrix is used to extend the concept of average linear velocity, i.e. the CoM velocity, to an average spatial velocity $\boldsymbol{v}_G$. An interesting property of the latter is that it allows to write the kinetic energy as the sum of the contribution due to the average spatial velocity itself and the internal motion of the robot. A similar separation of the terms constituting the kinetic energy can be obtained after the coordinate transformation that we have proposed. However, it is important to notice that our goal is not to come up with a generalization of the CoM velocity but to obtain, based on physical considerations, a coordinate transformation that leads to a simpler structure of the dynamic equations of motion. In our case the kinetic energy can be written as

$$T = \frac{1}{2}\left(\frac{1}{m}\boldsymbol{p}^T\boldsymbol{p} + \boldsymbol{l}^T\boldsymbol{\Lambda}_l(\boldsymbol{x})\boldsymbol{l} + \dot{\boldsymbol{q}}^T\boldsymbol{\Lambda}_q(\boldsymbol{x})\dot{\boldsymbol{q}}\right) \ , \qquad (34)$$

showing that for a multi-body system the term due to the relative internal motion needs to be added to the ones depending on the linear and angular momentum. The latter correspond to the term depending on the average spatial velocity in Orin et al. (2013).

5. APPLICATION

In Ott et al. (2011) the key point for the balancing strategy is to use the floating base model of the robot where the CoM position and velocity replace the corresponding floating base quantities, obtaining (omitting the dependencies)

$$\begin{aligned} \begin{bmatrix} m\boldsymbol{E}_3 & \boldsymbol{0} & \boldsymbol{0} \\ \boldsymbol{0} & \breve{\boldsymbol{M}}_{11} & \breve{\boldsymbol{M}}_{12} \\ \boldsymbol{0} & \breve{\boldsymbol{M}}_{12}^T & \boldsymbol{\Lambda}_q \end{bmatrix} \dot{\boldsymbol{v}}_C + \begin{bmatrix} \boldsymbol{0} \\ \breve{\boldsymbol{C}}_1\boldsymbol{v}_c \\ \breve{\boldsymbol{C}}_2\boldsymbol{v}_c \end{bmatrix} + \begin{bmatrix} m\,g\,\boldsymbol{e}_g \\ \boldsymbol{0} \\ \boldsymbol{0} \end{bmatrix} \\ = \begin{bmatrix} \boldsymbol{0} \\ \boldsymbol{0} \\ \boldsymbol{\tau} \end{bmatrix} + \sum_i \breve{\boldsymbol{J}}_i^T\boldsymbol{w}_i \end{aligned} \ , \qquad (35)$$

with $\boldsymbol{v}_c = \left[\,\dot{\boldsymbol{x}}_{CoM}^T \ \boldsymbol{\omega}_b^T \ \dot{\boldsymbol{q}}^T\,\right]^T$. The body angular velocity of the base link is denoted by $\boldsymbol{\omega}_b \in \mathbb{R}^3$ and the position of the CoM by $\boldsymbol{x}_{CoM} \in \mathbb{R}^3$, both expressed relative to the inertial frame. Finally, $\breve{\boldsymbol{J}}_i^T$ is the Jacobian matrix mapping the contact wrenches $\boldsymbol{w}_i$ to the generalized forces of the model, after the coordinate transformation.

Given the expression of the model in the new coordinates, the authors proposed to use a PD feedback law [2] for the desired wrench $\boldsymbol{w}_{CoM}^d$ acting at the CoM

$$\boldsymbol{w}_{CoM}^d = \begin{bmatrix} m\,g\,\boldsymbol{e}_g \\ \boldsymbol{0} \end{bmatrix} - \begin{bmatrix} \breve{\boldsymbol{K}}_P\tilde{\boldsymbol{x}}_{CoM} \\ \breve{\boldsymbol{\tau}}_P(\delta, \boldsymbol{\epsilon}) \end{bmatrix} - \begin{bmatrix} \breve{\boldsymbol{K}}_D\dot{\boldsymbol{x}}_{CoM} \\ \breve{\boldsymbol{D}}\boldsymbol{\omega}_b \end{bmatrix} \ , \qquad (36)$$

where the gain matrices $\breve{\boldsymbol{K}}_P$, $\breve{\boldsymbol{K}}_D$, $\breve{\boldsymbol{D}} \in \mathbb{R}^{3\times 3}$ are symmetric and positive definite. Additionally, $\boldsymbol{x}_{CoM}^d$ is the desired position of the CoM and $\tilde{\boldsymbol{x}}_{CoM} = \boldsymbol{x}_{CoM} - \boldsymbol{x}_{CoM}^d$, while $\breve{\boldsymbol{\tau}}_P$ represents the torque of a rotational spring connecting the frame attached to the base link to a fixed desired one. The torque is given by $\breve{\boldsymbol{\tau}}_P = -2(\delta\breve{\boldsymbol{K}}_R\boldsymbol{\epsilon} + \boldsymbol{\epsilon} \times \breve{\boldsymbol{K}}_R\boldsymbol{\epsilon})$ with $\breve{\boldsymbol{K}}_R$ symmetric and positive definite. The quantities δ and $\boldsymbol{\epsilon}$ specify the scalar and vector part of the quaternion representation of the rotational error $\boldsymbol{R}_B^{\Delta} = (\boldsymbol{R}_B^d)^T\boldsymbol{R}_B$ with $\boldsymbol{R}_B$ and $\boldsymbol{R}_B^d$ being the real and the desired orientation of the hip relative to the inertial frame. The choice is motivated by the identity

$$\sum_i \breve{\boldsymbol{J}}_{ib}^T\boldsymbol{w}_i = \boldsymbol{w}_{CoM} \ , \qquad (37)$$

where $\breve{\boldsymbol{J}}_i(\boldsymbol{x}) = \left[\breve{\boldsymbol{J}}_{ib}(\boldsymbol{x}) \ \ \breve{\boldsymbol{J}}_{iq}(\boldsymbol{x})\right]$. If contact wrenches that sum up exactly to the desired $\boldsymbol{w}_{CoM}^d$ can be produced, then from the first three lines of (35) we obtain a stable dynamics for the CoM. Although, for the base link orientation, the same can be concluded only if the terms $\breve{\boldsymbol{M}}_{12}(\boldsymbol{x})\ddot{\boldsymbol{q}}$ and some velocity dependent terms are assumed to be negligible. The desired contact wrenches $\boldsymbol{w}_i^d$ are computed through an optimization which (taking into account several restrictions concerning friction, the Center of Pressure and unilaterality of the contacts) solves (37) where $\boldsymbol{w}_{CoM}$ is replaced with (36). The desired contact wrenches are finally mapped quasi-statically to the joint torques by $\boldsymbol{\tau} = -\breve{\boldsymbol{J}}_{iq}^T\boldsymbol{w}_i^d$. Similar assumptions are made

[2] In case of nonredundant and nonsingular configurations for which the feet of the robot keep contact with the floor, the control law is a full state feedback.

in Henze et al. (2014), where they are used to obtain a simplified model from (35), which is then used for Model Predictive Control.

In order to reduce the effects of the assumptions necessary in the previous methods, we will propose a balancing controller which exploits the structure of (25). As in Ott et al. (2011), the optimization computes the desired contact wrenches $\boldsymbol{w}_i^d$ by solving

$$\sum_i \bar{\boldsymbol{J}}_{ib}^T \boldsymbol{w}_i^d = \boldsymbol{\Lambda}_h(\boldsymbol{x}) \left(\boldsymbol{w}_{CoM}^d - \begin{bmatrix} \bar{\boldsymbol{K}}_D & \boldsymbol{0} \\ \boldsymbol{0} & \bar{\boldsymbol{D}} \end{bmatrix} \boldsymbol{h} \right), \tag{38}$$

where $\bar{\boldsymbol{J}}_i(\boldsymbol{x}) = \left[\bar{\boldsymbol{J}}_{ib}(\boldsymbol{x}) \; \bar{\boldsymbol{J}}_{iq}(\boldsymbol{x}) \right]$ and the desired wrench at the CoM is

$$\boldsymbol{w}_{\mathrm{CoM}}^d = \begin{bmatrix} m\, g\, \boldsymbol{e}_g \\ \boldsymbol{0} \end{bmatrix} - \begin{bmatrix} \bar{\boldsymbol{K}}_P \tilde{\boldsymbol{x}}_{CoM} \\ \bar{\boldsymbol{\tau}}_P(\delta, \boldsymbol{\epsilon}) \end{bmatrix} \tag{39}$$

with $\bar{\boldsymbol{\tau}}_P = -2(\delta \bar{\boldsymbol{K}}_R \boldsymbol{\epsilon} + \boldsymbol{\epsilon} \times \bar{\boldsymbol{K}}_R \boldsymbol{\epsilon})$ and $\bar{\boldsymbol{K}}_R, \bar{\boldsymbol{K}}_D, \bar{\boldsymbol{D}} \in \mathbb{R}^{3\times3}$ symmetric positive definite matrices. Finally, the desired contact wrenches are also mapped quasi-statically to the joint torques as $\boldsymbol{\tau} = -\bar{\boldsymbol{J}}_{iq}^T \boldsymbol{w}_i^d$. Note that in (38) the velocity dependent term used in (36) has been replaced with a similar one expressed in terms of the generalized momentum. Nevertheless, interpreting $\boldsymbol{w}_{CoM}^d$ in (38) as the desired value of the derivative of the generalized momentum, we can guarantee that $\boldsymbol{h} \to \boldsymbol{0}$ as $t \to \infty$ whenever $\boldsymbol{w}_i^d$ can be produced exactly, since a first order dynamics in terms of the generalized momentum will be obtained.

The proposed balancing approach is evaluated in an experiment with the humanoid robot TORO described in Englsberger et al. (2014), which was developed at the German Aerospace Center (DLR). The robot has 27 degrees of freedom with a height of 1.7 m and a weight of about 77.5 kg.

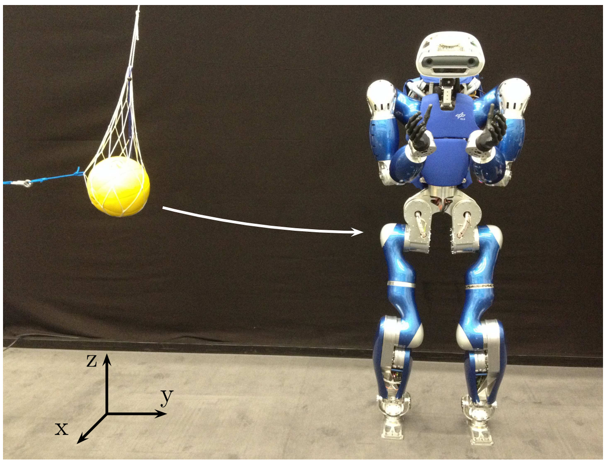

Fig. 1. Setup of the experiment

In the presented scenario, TORO is using its legs to maintain balance while being pushed to the side (see Fig. 1). The push is caused by a pendulum with a point mass of 5 kg, which hits the robot with a kinetic energy of 17.4 J at the hip. This impulsive disturbance causes the robot to perform a mainly lateral motion. The corresponding measurements, which are shown in Fig. 2, are given with respect to the inertial frame drawn in Fig. 1. The parameters used for the experiment are listed in Table 1. The the excitation of the CoM has a maximal amplitude of 0.045 m in the y-direction and a settling time of about 4.7 s. Referring to the error in the orientation, the maximal amplitude about the x-axis is 0.11 rad with a settling time of 4.7 s again. The plots for the linear and angular momentum are rather noisy due to some noise in the measurements of the joint velocities. Here, the maximal amplitude in the error is 14.5 kg·m/s for the linear momentum and 1.2 kg·m²/s for the angular momentum.

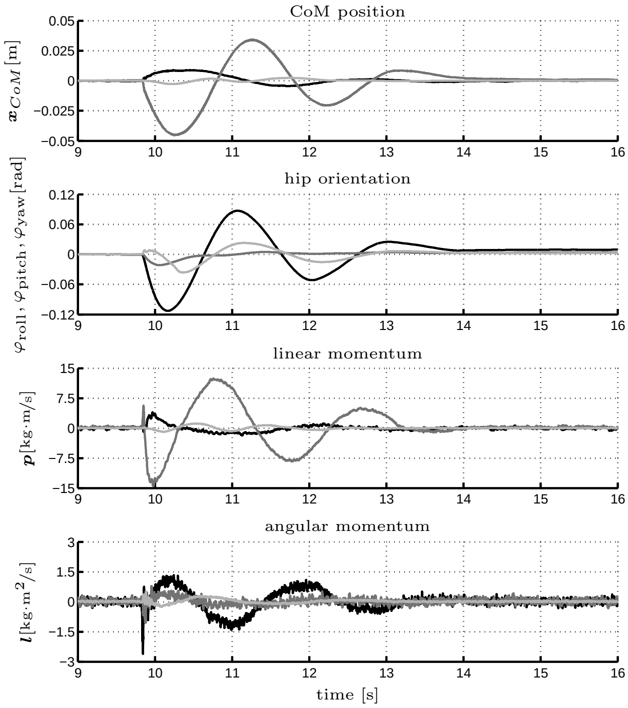

Fig. 2. Results of the experiment (black: x, dark gray: y, light gray: z)

Table 1. Parameters used for the experiment

Parameter	Value	Unit
$\boldsymbol{K}_P$	diag(6000, 2000, 4000)	N/m
$\bar{\boldsymbol{K}}_D$	diag(7, 1, 0.05)	N·s/kg·m
$\bar{\boldsymbol{K}}_R$	diag(500, 400, 100)	N · m
$\bar{\boldsymbol{D}}$	diag(20, 20, 2)	N·s/kg·m

The advantages of the proposed approach compared to the one presented in Ott et al. (2011), are given by the block diagonal structure of the transformed inertia matrix. Due to that, not only it is not required to neglect some terms of the model when considering the angular part of the desired wrench at the CoM, but the approach results especially promising for future extensions to a tracking controller. In this case, acceleration dependent terms, which would need to be taken into account in form of a compensation or a feedforward control, automatically vanish because of the structure of the equations.

6. CONCLUSION

A coordinate transformation that produces an inertially decoupled structure of the equations of motion of a floating base robot has been presented. The transformation is derived based on first principles of mechanics and therefore has a clear physical interpretation. The insights gained from the simpler structure can lead to more effective control laws. As an example, a balancing strategy has been proposed and simulated for a humanoid robot, which overcomes some minor problems of previous approaches and looks promising for extensions to the tracking case. In view of (19), additional future works aim at a different factorization of the Coriolis matrix which extends the inertial decoupling also to the velocity dependent terms.

REFERENCES

De Luca, A. and Flacco, F. (2011). A PD-type regulator with exact gravity cancellation for robots with flexible joints. In *IEEE Int. Conf. on Robotics and Automation (ICRA)*, 317–323. Shanghai, China.

Englsberger, J., Werner, A., Ott, C., Henze, B., Roa, M.A., Garofalo, G., Burger, R., Beyer, A., Eiberger, O., Schmid, K., and Albu-Schäffer, A. (2014). Overview of the torque-controlled humanoid robot TORO. In *IEEE/RAS Int. Conf. on Humanoid Robots*, 916–923. Madrid, Spain.

Garofalo, G., Ott, C., and Albu-Schäffer, A. (2013). On the closed form computation of the dynamic matrices and their differentiations. In *IEEE/RSJ Int. Conf. on Intelligent Robots and Systems (IROS)*. Tokyo, Japan.

Henze, B., Ott, C., and Roa, M.A. (2014). Posture and balance control for humanoid robots in multi-contact scenarios based on model predictive control. In *IEEE/RSJ Int. Conf. on Intelligent Robots and Systems (IROS)*, 3253–3258. Chicago, USA.

Hollerbach, J.M. (1980). A recursive Lagrangian formulation of maniputator dynamics and a comparative study of dynamics formulation complexity. *IEEE Trans. on Systems, Man and Cybernetics*, 10, 730–736.

Hyon, S.H., Hale, J.G., and Cheng, G. (2007). Full-body compliant human-humanoid interaction: Balancing in the presence of unknown external forces. *IEEE Trans. on Robotics*, 23(5), 884–898.

Kajita, S., Kanehiro, F., Kaneko, K., Fujiwara, K., Harada, K., Yokoi, K., and Hirukawa, H. (2003). Resolved momentum control: Humanoid motion planning based on the linear and angular momentum. In *IEEE/RSJ Int. Conf. on Intelligent Robots and Systems (IROS)*, 1644–1650. Las Vegas, USA.

Müller, A. (2007). Partial derivatives of the inverse mass matrix of multibody systems via its factorization. *IEEE Trans. on Robotics*, 23(1), 164–168.

Orin, D.E., Goswami, A., and Lee, S.H. (2013). Centroidal dynamics of a humanoid robot. *Autonomous Robots*, 35, 161–176.

Orin, D.E., McGhee, R., Vukobratovi, M., and Hartoch, G. (1979). Kinematic and kinetic analysis of open-chain linkage utilizing newton-euler methods. *Mathematical Biosciences*, 43, 107–130.

Ott, C. (2008). *Cartesian Impedance Control of Redundant and Flexible-Joint Robots*. Springer Tracts in Advanced Robotics. Springer-Verlag, Berlin.

Ott, C., Kugi, A., and Nakamura, Y. (2008). Resolving the problem of non-integrability of nullspace velocities for compliance control of redundant manipulators by using semi-definite Lyapunov functions. In *IEEE Int. Conf. on Robotics and Automation (ICRA)*, 1456–1463. Pasadena, USA.

Ott, C., Roa, M.A., and Hirzinger, G. (2011). Posture and balance control for biped robots based on contact force optimization. In *IEEE/RAS Int. Conf. on Humanoid Robots*, 26–33. Bled, Slovenia.

Silver, W.M. (1982). On the equivalence of Lagrangian and Newton-Euler dynamics for manipulators. *Int. Journal of Robotics Research*, 1, 60–70.

Sohl, G.A. and Bobrow, J.E. (2001). A recursive multibody dynamics and sensitivity algorithm for branched kinematic chains. *the ASME Journal of Dynamic Systems, Measurement, and Control*, 123, 391–399.

Spong, M.W. (1987). Modeling and control of elastic joint robots. *the ASME Journal of Dynamic Systems, Measurement, and Control*, 109, 310–318.

Stepanenko, Y. and Vukobratovic, M. (1976). Dynamics of articulated open-chain active mechanisms. *Mathematical Biosciences*, 28, 137–170.

Suleiman, W., Yoshida, E., Laumond, J.P., and Monin, A. (2008). Optimizing humanoid motions using recursive dynamics and Lie groups. In *International Conference on Information and Communication Technologies: from Theory to Applications (ICTTA)*, 1–6. Damascus, Syria.

Uicker, J.J. (1965). *On the Dynamic Analysis of Spatial Linkages Using 4x4 Matrices*. Ph.D. thesis, Northwestern University.

Umetani, Y. and Yoshida, K. (1987). Continuous path control of space manipulators mounted on OMV. *Acta Astronautica*, 15, 981–986.

Umetani, Y. and Yoshida, K. (1989). Resolved motion rate control of space manipulators with generalized Jacobian matrix. *IEEE Trans. Robotics and Automation*, 5, 303–314.

Vereshchagin, A.F. (1974). Computer simulation of the dynamics of complicated mechanisms of robot manipulators. *Engineering Cybernetics*, 6, 65–70.

Wieber, P.B. (2006). *Holonomy and Nonholonomy in the Dynamics of Articulated Motion*. Lecture Notes in Control and Information Sciences. Springer, Berlin.

Appendix A. PSEUDO-INVERSE OF THE CENTROIDAL MOMENTUM MATRIX

Due to the orthogonality relationship between $\boldsymbol{A}_p(\boldsymbol{x})$ and $\boldsymbol{A}_l(\boldsymbol{x})$ in (21), the pseudo-inverse of the centroidal momentum matrix $\boldsymbol{A}(\boldsymbol{x})^{+_M}$ can be expressed as

$$\begin{aligned}\boldsymbol{A}(\boldsymbol{x})^{+_M} &= \begin{bmatrix}\boldsymbol{A}_p(\boldsymbol{x})\\ \boldsymbol{A}_l(\boldsymbol{x})\end{bmatrix}^{+_M}\\ &= \boldsymbol{M}^{-1}(\boldsymbol{x})\begin{bmatrix}\boldsymbol{A}_p^T(\boldsymbol{x}) & \boldsymbol{A}_l^T(\boldsymbol{x})\end{bmatrix}\begin{bmatrix}\boldsymbol{\Lambda}_p(\boldsymbol{x}) & \boldsymbol{0}\\ \boldsymbol{0} & \boldsymbol{\Lambda}_l(\boldsymbol{x})\end{bmatrix}\\ &= \begin{bmatrix}\boldsymbol{A}_p^{+_M}(\boldsymbol{x}) & \boldsymbol{A}_l^{+_M}(\boldsymbol{x})\end{bmatrix} ,\end{aligned}$$

where (22) - (24) have been taken into account.